Subsolidus phase relations and crystal structure of compounds in the PrO_x–CaO–CuO system

G.B. Song,[a,b,*] C.Q. Han,[a] X.L. Chen,[a] J.K. Liang,[a,c] Q.L. Liu,[a] Y.Q. Zhou,[a] F.S. Liu,[a,b] and G.H. Rao[a]

[a] Institute of Physics and Center for Condensed Matter Physics, Chinese Academy of Sciences, Box 603, Beijing 100080, People's Republic of China
[b] School of Material Science and Engineering, Southwest University of Science and Technology, Mianyang 621002, People's Republic of China
[c] International Center for Materials Physics, Chinese Academy of Sciences, Shenyang 110016, People's Republic of China

Abstract

The subsolidus phase relations of the PrO_x–CaO–CuO pseudo-ternary system sintered at 950–1000°C have been investigated by X-ray powder diffraction. In this system, there exist one compound $Ca_{10}Pr_4Cu_{24}O_{41}$, one $Ca_2Pr_2Cu_5O_{10}$-based solid solution, seven three-phase regions and two two-phase regions. The crystal structures of $Ca_{10}Pr_4Cu_{24}O_{41}$ and $Ca_2Pr_2Cu_5O_{10}$-based solid solution have been determined. Compound $Ca_{10}Pr_4Cu_{24}O_{41}$ crystallizes in an orthorhombic cell with space group $D_{2h}^{20} - Cccm$, $Z = 4$. Its lattice parameters are $a = 11.278(2)$ Å, $b = 12.448(3)$ Å and $c = 27.486(8)$ Å. The crystal structure of $Ca_2Pr_2Cu_5O_{10}$-based solid solution is an incommensurate phase based on the orthorhombic $NaCuO_2$ type subcell. The lattice parameters of the subcell of the $Ca_{2.4}Pr_{1.6}Cu_5O_{10}$ are $a_0 = 2.8246(7)$ Å, $b_0 = 6.3693(5)$ Å, $c_0 = 10.679(1)$ Å, and those of the orthorhombic superstructure are with $a = 5a_0$, $b = b_0$, $c = 5c_0$. The $Ca_{2.4}Pr_{1.6}Cu_5O_{10}$ structure can also be determined by using a monoclinic supercell with space group $C_{2h}^5 - P2_1/c$, $Z = 4$, $a = 5a_0$, $b = b_0$, $c = c_0/\sin\beta$ and $\beta = 104.79(1)°$ or $136.60(1)°$, $V = 5a_0b_0c_0$.
© 2004 Elsevier Inc. All rights reserved.

1. Introduction

Since the discovery of high T_C oxide superconductors such as $La_{2-x}Ba_xCuO_4$ [1], $YBa_2Cu_3O_7$ [2,3], $YBa_2Cu_4O_8$ [4,5], and $Y_2Ba_4Cu_7O_{15}$ [4,6], a series of phase relations of R_2O_3−BaO−CuO systems (R = rare earth elements) have been extensively investigated for exploring new superconductors and for improving the synthesizing processes. In many systems isostructural superconductors $RBa_2Cu_3O_7$ (R = lanthanide elements except for Pm and Ce) [7], $RBa_2Cu_4O_8$ (R = Nd, Sm, Eu, Gd, Dy, Ho, Er, Tm) [8] and $R_2Ba_4Cu_7O_{15}$ (R = Eu, Gd, Dy, Ho, Er, Yb) [9,10] were found to exist. The phases $RBa_2Cu_4O_8$ and $R_2Ba_4Cu_7O_{15}$ were synthesized in high

oxygen pressure. Larger the radius of rare earth ions higher, the synthesizing oxygen pressure. However, the compound $PrBa_2Cu_3O_7$ does not exhibit superconducting properties. It is known that a partial substitution of Ca for Pr in $PrBa_2Cu_3O_7$ has a notable influence on its electronic transport properties. Superconductivity was observed in $Pr_{1-x}Ca_xBa_2Cu_3O_7$ ($x = 0.5$) synthesized under high pressures with transition temperature $T_C = 97−115$ K [11,12]. This shows that the Ca cations may play an important role in inducing the superconductivity. We had investigated in details the phase relations of PrO_x–BaO–CuO pseudo-ternary system, the solubility and the structure of $Pr_{1+x}Ba_{2-x}Cu_3O_7$ solid solutions [13]. In order to understand the effects of the Ca-ion and to find new functional materials in the Pr–Ca–Cu–O system, we study the phase relation and the crystal structure of compounds in PrO_x–CaO–CuO system (the content of oxygen and average valence of Pr may be varied in the synthesized process) by means of X-ray powder diffraction.

---

*Corresponding author. Institute of Physics and Center for Condensed Matter Physics, Chinese Academy of Sciences, Box 603, Beijing 100080, People's Republic of China. Fax: +861082649531.
E-mail addresses: gbsong@aphy.iphy.ac.cn (G.B. Song), jkliang@aphy.iphy.ac.cn (J.K. Liang).

2. Experimental

All samples of different compositions were synthesized by conventional solid-state reaction method in air. The purity of all starting materials Pr_6O_{11}, CuO and $CaCO_3$ is higher than 99.9 wt%. The dry raw powders with proper amounts were weighted, thoroughly mixed and ground in an agate mortar, and then pre-sintered in air at 850°C for about 12 h. The pre-sintered raw powders after regrinding and remixing were pressed into disks with a diameter of 10 mm and a thickness of 1–2 mm, and the disks were again sintered at 950–1000°C for 48 h in air, and then cooled in furnace to the room temperature. The above processes were repeated until homogeneity of samples was reached monitored by X-ray diffraction. Care was taken for the CaO-rich samples, since they were unstable and tended to form the basic calcium carbonate after absorbing the carbon dioxide and water in air. The CaO-rich samples after preparing must be kept in a desiccator before using for X-ray diffraction experiments. 58 samples of PrO_x–CaO–CuO system were prepared and their compositions are shown in Fig. 1.

X-ray powder diffraction data were collected on a Rigaku Rint 2500 X-ray diffractometer (200 mA × 40 kV) with CuKα radiation and a graphite monochromator. The data for structural analysis and accurate determination of lattice parameters were recorded by a step scan mode with a scanning step of $2\theta = 0.02°$ and a sampling time of 2 s. Pure Si was added to the samples as an internal standard. The phase identifications were carried out by the continuous scan mode with a rate of $2\theta = 4°$/min.

The electron diffractions of some samples were carried out by transmission electron microscopy (TEM). These specimens were ground under acetone and dispersed on to holey carbon grids. The electron diffraction patterns were collected by using a H-9000 NA TEM at 300 kV.

3. Results and discussion

3.1. Subsolidus phase relations

In the PrO_x–CuO system, two compounds $PrCuO_2$ and Pr_2CuO_4 were reported. Compound $PrCuO_2$ [14], which was synthesized by using starting materials Cu_2O and Pr_2O_3 in reducing atmosphere, belongs to a trigonal system with space group $R\bar{3}m$ and its lattice parameters $a = 3.75$ Å, and $c = 17.09$ Å. Compound Pr_2CuO_4 crystallizes in a tetragonal unit cell with space group $I4/mmm$ and K_2NiF_4 type structure [15], its lattice parameters are $a = 3.963$ Å, and $c = 12.233$ Å. Under our experimental conditions only compound Pr_2CuO_4 was identified. Its lattice parameters $a = 3.961(2)$ Å, and $c = 12.214(6)$ Å are consistent with the previously reported values [15].

In the PrO_x–CaO system, no compound was observed in our investigation and was reported previously. Tikhonov et al. studied the effect of CaO doping on electro-conductivity in Y_2O_3–PrO_x system [16].

In the CaO–CuO system, two compounds Ca_2CuO_3 and $CaCu_2O_3$ were prepared at the atmospheric pressure [17] and one more compound $CaCuO_{2-\delta}$ can be synthesized under high-pressure conditions [18]. Ca_2CuO_3 belongs to an orthorhombic system with space group *Immm* and its lattice parameters are $a = 12.239$ Å, $b = 3.779$ Å and $c = 3.259$ Å. Compound $CaCu_2O_3$ also possesses an orthorhombic unit cell with space group *Pmmm* and its lattice parameters are $a = 9.85$ Å, $b = 4.11$ Å and $c = 3.47$ Å [17]. Under our experiment conditions only one compound, Ca_2CuO_3, was identified. These results coincide with the previous report [19] and collection of phase diagrams for ceramists [20]. After indexing Ca_2CuO_3, its structure is confirmed to be the same as the reported one [17]. Its lattice parameters are $a = 12.208(6)$ Å, $b = 3.768(2)$ Å and $c = 3.249(2)$ Å.

Phase identification of samples in the pseudo-ternary system PrO_x–CaO–CuO was carried out by X-ray powder diffraction. The solid solubility was determined by means of disappearing-phase method. The subsolidus phase relations of PrO_x–CaO–CuO pseudo-ternary system under our synthesizing condition are shown in Fig. 1. There exist one compound, $Ca_{10}Pr_4Cu_{24}O_{41}$, and one solid solution based on composition $Ca_2Pr_2Cu_5O_{10}$.

Compound $Ca_{10}Pr_4Cu_{24}O_{41}$ belongs to an orthorhombic system with space group $D_{2h}^{20} - Cccm$. $Ca_2Pr_2Cu_5O_{10}$ is an incommensurate phase based on the orthorhombic $NaCuO_2$-type subcell [21–23]. The
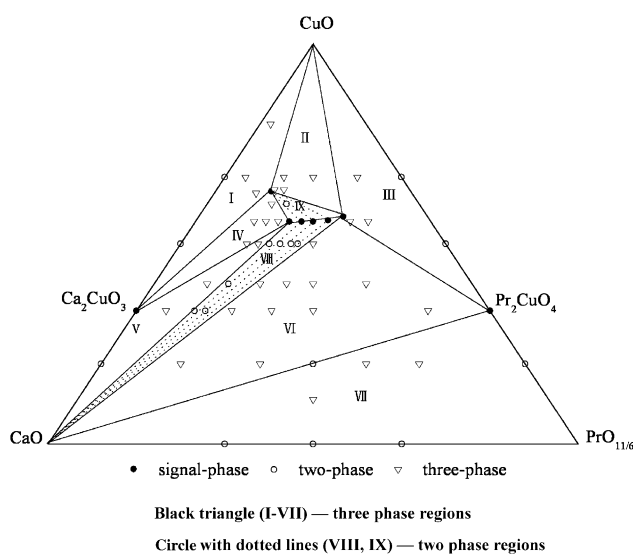

Fig. 1. Subsolidus phase relation of PrO_x–CaO–CuO pseudo-ternary system.

result of phase identification according to XRD data shows that the sample with the nominal composition $Ca_{1.8}Pr_{2.2}Cu_5O_{10}$ in our synthesizing condition consists of two phases: $Ca_2Pr_2Cu_5O_{10}$-based solid solution and trace CaO, while the sample with nominal composition $Ca_{1.6}Pr_{2.4}Cu_5O_{10}$ contains three phases: $Ca_2Pr_2Cu_5O_{10}$-based solid solution, very little of CaO and Pr_2CuO_4 (see Fig. 3). Based on the charge neutrality and the disappearing-phase method, the solid solubility of the $Ca_2Pr_2Cu_5O_{10}$-based solid solution can be determined to range from about $Ca_{2.4}Pr_{1.6}Cu_5O_{10}$ (partial Pr^{3+} or/and Cu^{2+} are changed to Pr^{4+} or/and Cu^{3+}, respectively) to about $Ca_{3/2}Pr_{7/3}Cu_5O_{10}$ (the content of oxygen cannot exceed 10 in a formula unit and the valence of Pr or Cu cannot be less than Pr^{3+} or Cu^{2+}, respectively), according to CaO similar diffraction intensity for both samples $Ca_{1.8}Pr_{2.2}Cu_5O_{10}$ and $Ca_{1.6}Pr_{2.4}Cu_5O_{10}$ (see Fig. 3): $Ca_{1.8}Pr_{2.2}Cu_5O_{10} = Ca_{1.7}Pr_{2.2}Ca_5O_{10} + 0.1\,CaO$ and $Ca_{1.6}Pr_{2.4}Cu_5O_{10} = 0.991\,Ca_{3/2}Pr_{7/3}Cu_5O_{10} + 0.113\,CaO + 0.045\,Pr_2CuO_4$.

The subsolidus phase relation of PrO_x–CaO–CuO system under our synthesizing condition is shown in Fig. 1. It contains one compound $Ca_{10}Pr_4Cu_{24}O_{41}$ and one $Ca_2Pr_2Cu_5O_{10}$-based solid solution, and can be divided into 7 three-phase regions (I–VII) and 2 two-phase regions (VIII and IX).

3.2. Crystal structure of $Ca_{10}Pr_4Cu_{24}O_{41}$

Due to the similarity of chemical formula and XRD pattern between $Ca_{10}Pr_4Cu_{24}O_{41}$ and $Sr_{14-x}Ca_xCu_{24}O_{41}$ compounds, the XRD pattern collected 2θ from 10° to 120° of $Ca_{10}Pr_4Cu_{24}O_{41}$ was successfully indexed by way of trial and error method program [24]. The d-spacings and 2θ in the range $10° < 2\theta < 73°$ are listed in Table 1. It belongs to an orthorhombic system with lattice constants $a = 11.278(2)$ Å, $b = 12.448(3)$ Å and $c = 27.486(7)$ Å. The reflection conditions are: $h + k = 2n$ for (hkl), $k, l = 2n$ for (0kl) and $h, l = 2n$ for (h0l), from which one infers that the unit cell is an orthorhombic C-centered lattice and the possible space group is $D_{2h}^{20} - Cccm$ or $C_{2v}^{13} - Ccc2$.

The XRD pattern indicates that the $Ca_{10}Pr_4Cu_{24}O_{41}$ is isostructural to $Sr_{14-x}Ca_xCu_{24}O_{41}$ with space group Cccm [25]. The number of formula unit per unit cell in $Ca_{10}Pr_4Cu_{24}O_{41}$ structure is 4, i.e., a unit cell contains $40Ca + 16Pr + 96Cu + 164O$. The ideal atomic distributions on $y = 0, \frac{1}{8}, \frac{1}{4}, \frac{3}{8}, \frac{1}{2}, \frac{5}{8}, \frac{3}{4}, \frac{7}{8}$ sections are shown in Fig. 2. In the structural refinement, the oxygen atoms are fixed to their ideal positions because of their smaller atomic scattering power, and the temperature factors were taken as 1 Å², 0.7 Å², 0.7 Å² and 0.5 Å² for O, Cu, Ca and Pr, respectively. The atomic parameters of all cations are refined by the Rietveld method using DBWS-9411 program [26]. The final atomic parameters of all ions are listed in Table 2 with $R_p = 6.5\%$,

Table 1
Observed and calculated $2\theta_{obs}$, d_{obs}, $2\theta_{calc}$, d_{calc} and intensities I_{obs}, I_{calc} of $Ca_{10}Pr_4Cu_{24}O_{41}$

h k l	$2\theta_{obs}$	d_{obs}	$2\theta_{calc}$	d_{calc}	I_{obs}	I_{calc}
0 2 0	14.22	6.222	14.22	6.224	7	7
2 0 0	15.72	5.632	15.70	5.639	2	2
2 0 4	20.53	4.322	20.36	4.359	2	8
2 2 0	21.22	4.183	21.24	4.179	2	5
1 3 1	23.29	3.817	23.05	3.855	2	3
1 3 3	24.85	3.580	24.82	3.584	2	2
2 0 6	25.09	3.547	25.02	3.556	2	3
1 1 7			25.04	3.554		3
3 1 3	26.60	3.348	26.58	3.351	2	4
0 4 0	28.66	3.112	28.66	3.112	48	29
0 4 4			31.53	2.835		3
4 0 0	31.68	2.822	31.70	2.820	7	8
1 3 7	32.34	2.766	32.35	2.765	47	65
2 4 0	32.84	2.725	32.84	2.725	100	100
3 1 7	33.77	2.652	33.76	2.653	39	66
1 1 10	34.25	2.616	34.32	2.611	3	6
4 2 0	34.92	2.567	34.91	2.568	10	13
2 4 4	35.52	2.525	35.41	2.533	2	4
1 1 11	37.51	2.396	37.54	2.394	2	2
1 5 3	38.30	2.348	38.27	2.350	2	2
0 4 8	38.94	2.311	39.03	2.306	2	1
3 3 7	39.69	2.269	39.64	2.272	2	1
1 3 10	40.00	2.252	40.11	2.246	2	4
3 1 10	41.19	2.190	41.30	2.184	5	2
2 4 8	42.40	2.130	42.30	2.135	2	1
4 4 0	43.25	2.090	43.25	2.090	15	15
1 5 7	43.74	2.068	43.76	2.067	23	27
4 4 4	45.31	2.000	45.33	1.999	2	2
0 0 14	46.21	1.963	46.21	1.963	12	21
3 3 10	46.61	1.947	46.61	1.947	8	11
6 0 0	48.38	1.880	48.38	1.88	12	10
0 2 14	48.51	1.875	48.60	1.872	7	11
2 0 14	49.01	1.857	48.99	1.858	2	2
1 5 10	50.02	1.822	50.05	1.821	2	2
6 2 0	50.67	1.800	50.70	1.799	14	20
2 2 14	51.41	1.776	51.38	1.777	2	2
5 3 7	51.59	1.770	51.63	1.769	15	15
4 6 0	55.04	1.667	54.90	1.671	4	4
3 5 10	55.33	1.659	55.44	1.656	3	6
5 3 10	57.44	1.603	57.24	1.608	5	6
2 4 14	57.83	1.593	57.83	1.593	10	16
0 8 0	59.35	1.556	59.35	1.556	21	18
5 5 7	60.11	1.538	60.11	1.538	5	9
3 7 7	62.35	1.488	62.35	1.488	14	11
4 4 14	65.13	1.431	65.13	1.431	12	12
5 5 10	65.29	1.428	65.29	1.428	5	4
0 6 14	65.44	1.425	65.39	1.426	3	4
8 0 0	66.23	1.410	66.23	1.410	2	3
7 3 7	66.60	1.403	66.60	1.403	4	8
6 6 0	67.14	1.393	67.14	1.393	8	8
8 2 0	68.14	1.375	68.14	1.375	4	4
4 8 0	68.88	1.362	68.88	1.362	2	2
6 0 14	69.11	1.358	69.11	1.358	9	11
0 2 20	69.94	1.344	70.06	1.342	2	2
6 2 14	71.03	1.326	70.97	1.327	6	6
7 3 10	71.59	1.317	71.53	1.318	4	1
2 2 20	72.29	1.306	72.35	1.305	2	2

Note: The relative intensities less than 2% in the region $10° < 2\theta < 73°$ are not listed in this table.
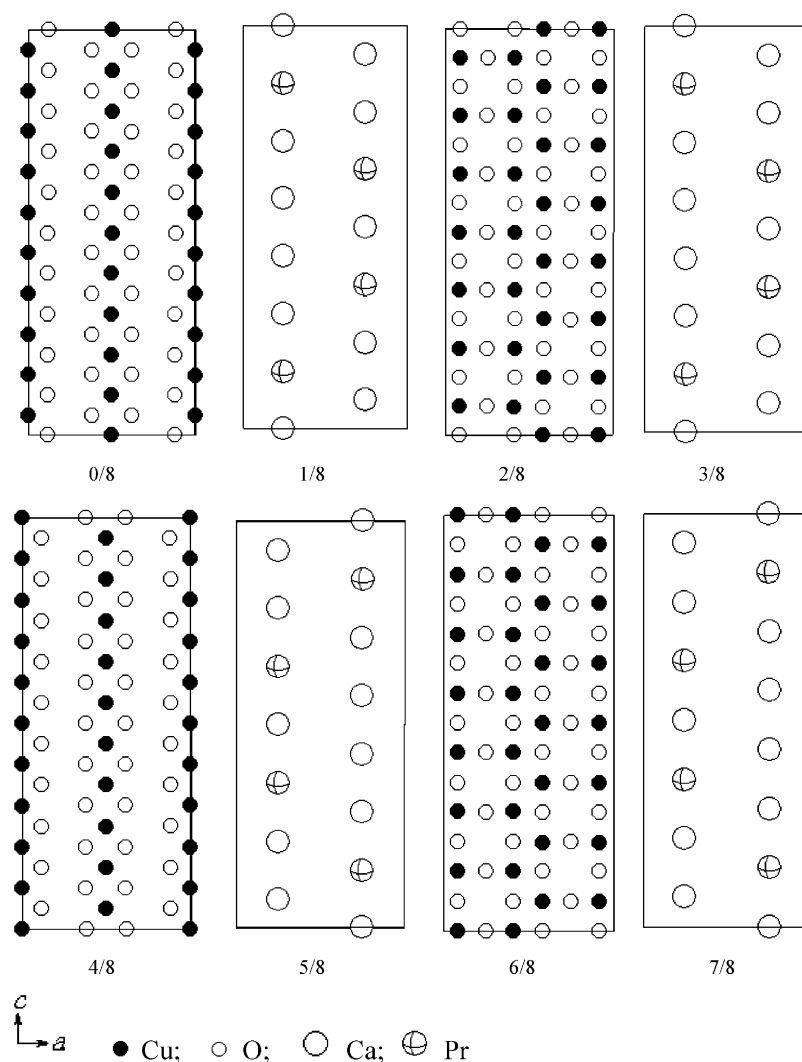
Fig. 2. Structure of $Ca_{10}Pr_4Cu_{24}O_{41}$ along b-axis at different y sections.

$R_{wp} = 8.96\%$ and $R_{exp} = 2.25\%$. The diffraction intensities calculated by the LAZY program according to the above-refined atomic parameters (see Table 2) are also listed in Table 1 for comparison with observed intensities, in which the diffraction peaks with intensities below 2/100 in the pattern are not included. As shown in Table 1 for $2\theta < 73°$ the calculated and the observed intensities I and planar distances d basically coincide with each other. It shows that the structure of $Ca_{10}Pr_4Cu_{24}O_{41}$ is correct. From the refined results listed in Table 2, we can evaluate the bond–valence of ions according to the interionic distance between cation and oxygen by Brown's empirical bond–valence method [27,28]. They are also listed in Table 2. The bond–valences of Pr, Ca, Cu and O are about 2.95, 1.97–2.01, 1.95–2.17 and 1.85–2.25, respectively. The above results indicate that the structure model and the atomic parameters are reasonable.

The structure of $Ca_{10}Pr_4Cu_{24}O_{41}$, which is considered as a commensurate phase, is better described as two

interpenetrating subcells: one with (Ca, Pr) layer—$(CuO_{3/3}O_{1/2})$ sheets—(Ca, Pr) layer in an orthorhombic subcell with dimensions of $a = 11.278(2)$ Å, $b = 12.448(3)$ Å, $c(s) = 3.9266(1)$ Å, and the other subcell with layers of the infinite $[CuO_{4/2}]$ chains also in an orthorhombic cell having identical a and b, but with $c(c) = 2.7486(1)$ Å. The coordination numbers Cu by oxygen in two subcells are both 4. The difference of the two subcells lies in the manner of linkage of the square planar cupper oxygen units. In the former case they form planes perpendicular to b-axis, and in the latter case they form infinite chain along the c-axis. They are then connected to one another via a layer of (Ca, Pr) ions. These two subcells combine to form the commensurate phase $Ca_{10}Pr_4Cu_{24}O_{41}$ at $7c(s)$ (sheet) = 27.486 Å and $10c(c)$(chain) = 27.486 Å. Therefore the X-ray diffraction pattern for $Ca_{10}Pr_4Cu_{24}O_{41}$ exhibit strong reflections with $l = 7n$ or $10n$.

The lattice parameters of $Sr_8Ca_6Cu_{24}O_{41}$ are $a = 11.375$ Å, $b = 12.927$ Å, $c = 27.453$ Å, and among them

Table 2
Refined and ideal atomic parameters of $Ca_{10}Pr_4Cu_{24}O_{41}$

Atoms	Wyckoff position	x	y	z	ΣV
Pr	16m	0.2570 (0.250)	0.1274 (0.125)	0.1350 (0.143)	2.95
Ca(1)	16m	0.7510 (0.750)	0.1305 (0.125)	0.0725 (0.072)	1.98
Ca(2)	16m	0.7527 (0.750)	0.1259 (0.125)	0.2299 (0.214)	1.97
Ca(3)	8l	0.2387 (0.250)	0.1362 (0.125)	0.000	2.01
Cu(1)	16m	0.0845 (0.086)	0.2553 (0.250)	0.0716 (0.071)	2.03
Cu(2)	16m	0.0858 (0.086)	0.2502 (0.250)	0.2178 (0.213)	2.06
Cu(3)	16m	0.0880 (0.086)	0.2431 (0.250)	0.3560 (0.357)	2.05
Cu(4)	8l	0.9135 (0.914)	0.2261 (0.250)	0.000	1.95
Cu(5)	8i	0.000	0.000	0.0617 (0.050)	2.12
Cu(6)	8i	0.000	0.000	0.1570 (0.150)	2.13
Cu(7)	8j	0.500	0.000	0.1224 (0.100)	2.04
Cu(8)	8j	0.500	0.000	0.1894 (0.200)	2.12
Cu(9)	4d	0.500	0.000	0.000	1.98
Cu(10)	4a	0.000	0.000	0.250	2.17
O(1)	16m	(0.086)	(0.250)	(0.143)	2.25
O(2)	16m	(0.086)	(0.250)	(0.286)	2.13
O(3)	16m	0.086	0.250	(0.429)	2.07
O(4)	8l(xy0)	(0.086)	(0.250)	0.000	2.09
O(5)	8k	0.250	0.250	(0.071)	1.85
O(6)	8k	0.250	0.250	(0.214)	2.10
O(7)	8k	0.250	0.250	(0.357)	2.05
O(8)	4f	0.750	0.250	0.000	2.02
O(9)	16m	(0.118)	(0.000)	(0.100)	1.98
O(10)	16m	(0.118)	(0.000)	(0.200)	1.95
O(11)	16m	(0.382)	(0.000)	(0.050)	2.06
O(12)	16m	(0.382)	(0.000)	(0.150)	1.91
O(13)	8g	(0.382)	0.000	0.250	2.02
O(14)	8l	(0.118)	0.000	0.000	2.17

Note: (1) The occupancies of all atoms are 1; (2) the temperature factors of Pr, Ca, Cu and O are fixed at $0.5\,\text{Å}^2$, $0.7\,\text{Å}^2$, $0.7\,\text{Å}^2$ and $1\,\text{Å}^2$, respectively; (3) the ideal positions of atoms are shown in the parentheses; (4) ΣV present bond valences of ions.

a and b are slightly larger than that of $Ca_{10}Pr_4\,Cu_{24}O_{41}$, while c is near to that of $Ca_{10}Pr_4\,Cu_{24}O_{41}$. It is known from its structure (see Fig. 2), the dimension of c is only related to CuO_4 chains and sheets, and a and b (specially b) are notably dependent with the dimension of atoms, while ionic radius of Sr^{2+} is larger than that of Pr^{3+} or Ca^{2+}.

3.3. Crystal structure of $Ca_2Pr_2Cu_5O_{10}$-based solid solution

The crystal structure of $Ca_2Pr_2Cu_5O_{10}$ is an incommensurate one based on the orthorhombic $NaCuO_2$-type structure, and isostructural to $Ca_2R_2Cu_5O_{10}$ ($R = Y$, Nd, Sm, Gd, Tm) [29,30]. The space group of the fundamental subcell is *Fmmm*. Davies [29] described the structure of $Ca_2R_2Cu_5O_{10}$ ($R = Y$, Nd, Gd) in detail, and deduced the relationship between the incommensurate orthorhombic subcell and the commensurated superstructure belonging to the orthorhombic or the monoclinic systems.

In order to keep a constant oxygen content as 10 atoms in one formula unit and the valence of Pr as Pr^{3+} or Pr^{4+} in the homogeneous range of $Ca_2Pr_2Cu_5O_{10}$-based solid solution, in the Ca-rich region (i.e.,

Ca/Pr > 1), the composition of solid solution can be expressed as a general formula $Ca_{2+x}Pr_{2-x}Cu_5O_{10}$, and in the Pr-rich region (i.e., Ca/Pr < 1) as $Ca_{3y/2}Pr_{(10-3y)/3}Cu_5O_{10}$.

The X-ray powder diffraction patterns of samples $Ca_{2+\delta}Pr_{2-\delta}Cu_5O_{10}$ with $\delta = 0.4$, 0.2, 0, -0.2 and -0.4 are shown in Fig. 3. From Fig. 3, one can see that one set of diffraction peaks change their positions slightly and can be indexed using an orthorhombic cell with space group *Fmmm*. With increasing of Pr content, the other set of the reflections, as indicated by "s", vary their positions considerably, and their distance between the pair of diffraction lines "s" decreases. These reflections cannot be indexed by using conventional method, but can be indexed by using fractional Miller indexes for h and l based on the lattice parameters of subcell. According to Davis' structural model [29], the first pair of incommensurate reflections observed close to $2\theta = 30°$ can be indexed as $(1-\delta h, 1, 1-\delta l)$ and $(1-\delta h, 1, 1+\delta l)$, the second pair of incommensurate reflections situated around $2\theta = 38°$ can be indexed as $(1-\delta h, 1, 3-\delta l)$ and $(1-\delta h, 1, 3+\delta l)$ and the third pair of incommensurate reflections observed close to $2\theta = 51°$ can be indexed as $(1-\delta h, 3, 1-\delta l)$ and $(1-\delta h, 3, 1+\delta l)$, respectively. The positions of incommensurate reflections

were used to calculate δh and δl:

$$\delta l = (c^2/4)(1/d^2_{(1-\delta h,1,1+\delta l)} - 1/d^2_{(1-\delta h,1,1-\delta l)}),$$

$$\delta l = (c^2/4)(1/d^2_{(1-\delta h,3,1+\delta l)} - 1/d^2_{(1-\delta h,3,1-\delta l)}),$$

or

$$\delta l = (c^2/12)(1/d^2_{(1-\delta h,1,3+\delta l)} - 1/d^2_{(1-\delta h,1,3-\delta l)})$$

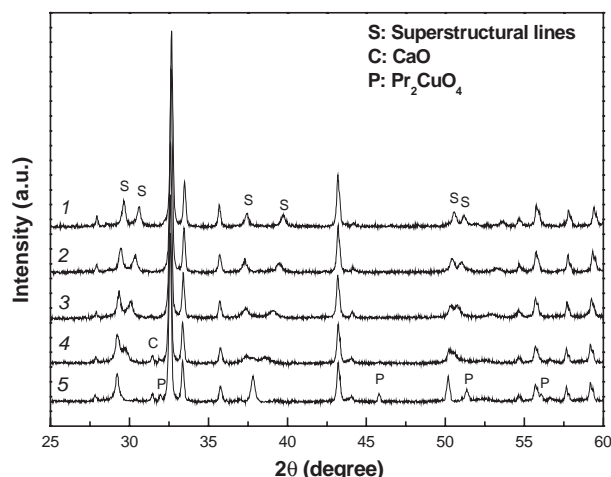Fig. 3. The X-ray powder diffraction patterns of samples with following compositions: (1) $Ca_{2.4}Pr_{1.6}Cu_5O_{10}$; (2) $Ca_{2.2}Pr_{1.8}Cu_5O_{10}$; (3) $Ca_2Pr_2Cu_5O_{10}$; (4) $Ca_{1.8}Pr_{2.2}Cu_5O_{10}$; and (5) $Ca_{5/3}Pr_{7/3}Cu_5O_{10}$.

δh was subsequently calculated from the positions of the individual incommensurate diffraction lines. The subcell parameters and δh, δl for the solid solution with different composition are listed in Table 3.

To confirm the validity of the indexing and lattice parameters described above, several samples were investigated by using electron diffraction method. Fig. 4 shows the electron diffraction pattern of $Ca_{2.4}Pr_{1.6}Cu_5O_{10}$ along the [010] axis of the subcell. The rectangle presented by thin lines and parallelogram by thick lines correspond to the reciprocal orthorhombic subcell and monoclinic supercell, respectively. For the orthorhombic subcell there exist some superstructure satellite reflections around each of the fundamental reflections. They can all be indexed by using of fractional Miller indices as $(h_0 \pm n\delta h, k_0, l_0 \pm n\delta l)$ for h_0, k_0, $l_0 = n + 1$ and $(h_0 \pm 2n\delta h, k_0, l_0 \pm 2n\delta l)$ for h_0, k_0, $l_0 = 2n$, where h_0, k_0, l_0 are Miller indices of the subcell and $\delta h = 0.2$, $\delta l = 0.2$ for $Ca_{2.4}Pr_{1.6}Cu_5O_{10}$. For example, around the transmitted beam (000) the superstructure satellite spots correspond to $(\pm 2\delta h, 0, \pm 2\delta l)$, i.e. $(\pm 0.4, 0, \pm 0.4)$, and around the (202) fundamental reflection, to $(2 \pm 2\delta h, 0, 2 \pm 2\delta l)$. The ratio c_0/a_0 of the subcell and δh, δl derived from Fig. 4 coincide with the results obtained by X-ray powder diffraction. It shows that the indexing results by the orthorhombic subcell

Table 3
Lattice parameters of subcell and supercell for $Ca_2Pr_2Cu_5O_{10}$ based solid solution

Composition	$Ca_{2.4}Pr_{1.6}Cu_5O_{10}$	$Ca_{2.2}Pr_{1.8}Cu_5O_{10}$	$Ca_2Pr_2Cu_5O_{10}$	$Ca_{1.7}Pr_{2.2}Cu_5O_{10}$	$Ca_{3/2}Pr_{7/3}Cu_5O_{10}$
Orth. subcell					
a_0 (Å)	2.8246(7)	2.8252(7)	2.8257(7)	2.8176(7)	2.8143(7)
b_0 (Å)	6.3693 (5)	6.381(1)	6.392(1)	6.390(1)	6.392(1)
c_0 (Å)	10.679 (4)	10.698(1)	10.718(1)	10.718(1)	10.720(1)
V_0 (Å³)	192.13	192.86	193.59	192.97	192.84
δh	0.2	0.2	0.2	0.2	0.2
δl	0.2	0.185	0.15	0.1	0
Orth. supercell					
a (Å)	$5\,a_0$	$5\,a_0$	$5\,a_0$	$5\,a_0$	$5\,a_0$
b (Å)	b_0	b_0	b_0	b_0	b_0
c (Å)	$5\,c_0$	$5.4\,c_0$	$6.67\,c_0$	$10\,c_0$	c_0
V (Å³)	$25\,V_0$	$27\,V_0$	$33.3\,V_0$	$50\,V_0$	$5\,V_0$
Monoc. supercell					
a (Å)	14.123(2)	14.126(4)	14.129(4)	14.088(4)	14.071(4)
b (Å)	6.3693 (5)	6.381 (1)	6.392 (1)	6.390 (1)	6.392 (1)
c (Å)					
A	11.045(1)	11.012(2)	10.925(2)	10.807(2)	
					10.720(2)
B	15.543(1)	15.715(2)	16.096(1)	16.602(1)	
β (°)					
A	104.79(1)	103.73(1)	101.18(1)	97.35(1)	
					90*
B	136.60(1)	137.10(1)	138.25(1)	139.79(1)	
V (Å³)	960.61($5\,V_0$)	964.25($5\,V_0$)	967.94($5\,V_0$)	964.88($5\,V_0$)	964.18($5\,V_0$)

Note: *In the general it must be expressed as orthorhombic supercell whose volume of unit cell is same to one of monoclinic supercell.
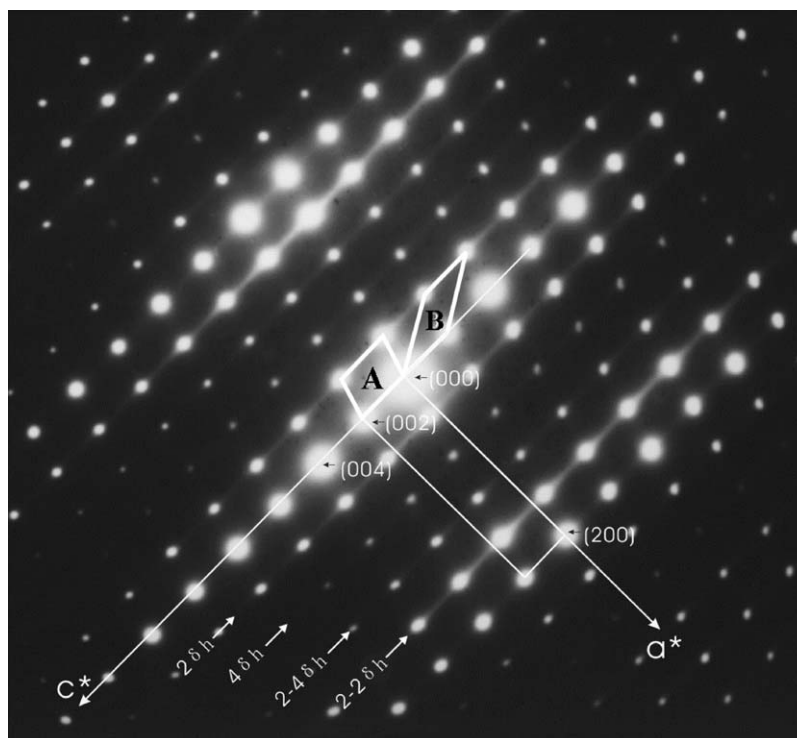
Fig. 4. The electron diffraction pattern of $Ca_{2.4}Pr_{1.6}Cu_5O_{10}$ along b-axis.

Table 4
Observed and calculated spacings d and intensities of $Ca_{2.4}Pr_{1.6}Cu_5O_{10}$

No.	d_{calc} (Å)	d_{obs} (Å)	I_{obs}	I_{calc}	Subcell	Orthorhombic supercell	Monoclinic supercell (hkl)	
					hkl	hkl	"A"	"B"
1	3.184	3.184	4	5	0 2 0	0 2 0	0 2 0	0 2 0
2	3.008	3.006	13	23	0.8 1 0.8	4 1 4	4 1 0	4 1 4̄
3	2.916	2.914	13	15	0.8 1 1.2	4 1 6	4 1 2̄	4 1 2
4	2.735	2.735	100	100	0 2 2	0 2 10	0 2 2	0 2 2
5	2.670	2.669	24	25	0 0 4	0 0 20	0 0 4	0 0 4̄
6	2.509	2.509	12	13	1 1 1	5 1 5	5 1 0, 5 1 2̄	5 1 3̄, 5 1 5̄
7	2.399	2.397	8	11	0.8 3 2.8	4 1 14	4 1 2	4 1 6
8	2.266	2.266	9	6	0.8 1 3.2	4 1 16	4 1 4̄	4 1 0̄
9	2.090	2.090	27	18	1 1 3	5 1 15	5 1 2, 5 1 4̄	5 1 1̄, 5 1 7̄
10	2.046	2.046	2	6	0 2 4	0 2 20	0 2 4	0 2 4̄
11	1.802	1.802	10	10	0.8 3 0.8	4 3 4	4 1 4, 4 3 0	4 1 8̄, 4 3 4
12	1.782	1.782	8	4	0.8 3 1.2	4 3 6	4 3 2̄	4 3 2
13	1.710	1.709	3	2	0.8 1 5.2	4 1 26	4 1 6	4 1 2̄
14	1.704	1.704	2	1	1 0 5	5 0 25	5 0 6, 5 0 6̄, 3 1 5	8 0 8̄
15	1.676	1.676	5	7	1 3 1	5 3 5	5 3 0, 5 3 2̄	5 3 3̄, 5 3 5̄
16	1.646	1.645	15	4	1 1 5	5 1 25	5 1 4, 5 1 6, 4 3 2	5 1 1, 5 1 6, 4 3 6̄
17	1.592	1.592	10	10	0 4 0	0 4 0	0 4 0	0 4 0
18	1.554	1.553	12	13	0 2 6	0 2 30	0 2 6,	0 2 6̄
19	1.532	1.532	7	1	1 3 3	5 3 15	5 3 2, 5 3 4̄	5 3 1̄, 5 3 7̄

Note: The relative intensities less than 2% in region $25° < 2\theta < 60°$ are not listed in this table.

shown in Table 4 are correct. For the monoclinic supercell there exist two selections: "A" and "B" as shown in Fig. 4. The monoclinic supercell "A" and "B" have the same unit cell volume, but different angle β. For the monoclinic supercell "A", $\beta = 180° - \tan^{-1}(c\,\delta h/a\,\delta l)$ and for the monoclinic supercell "B", $\beta = 180° - \tan^{-1}(c\,\delta h/a(1 - \delta l))$.

The lattice constants of monoclinic supercell are related to subcell parameters: $a_{mon} = a_{sub}/\delta h$, $b_{mon} = b_{sub}$, $c_{mon} = c_{sub}/\sin\beta$. All reflections can also be indexed using monoclinic supercell. The lattice parameters of monoclinic supercell are also listed in Table 3. From Table 3 one can see that with the increasing of Pr content the subcell parameter δh remains constant (0.2),
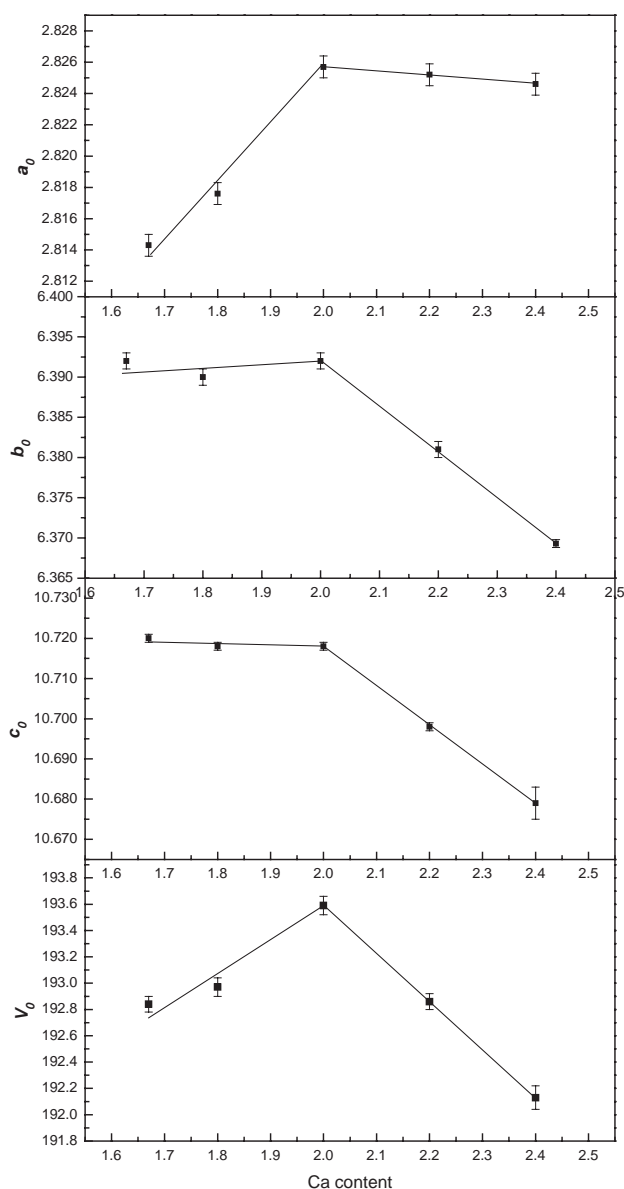
Fig. 5. Variation of subcell lattice parameters of solid solution based on $Ca_2Pr_2Cu_5O_{10}$ samples with Ca content.

$Ca_{2+x}Pr_{2-x}Cu_5O_{10}$ the substitution of Ca^{2+}-ion for Pr^{3+}-ion results in forming Cu^{3+} or Pr^{4+} ions to obtain a valence neutralization in the solid solution $Ca_{2+x}Pr_{2-x}Cu_5O_{10}$, the volume of unit cell decreased with increasing the concentration of Cu^{3+} or Pr^{4+}, because the ionic radii of Cu^{3+} and Pr^{4+} ion are smaller than those of the Cu^{2+} and Pr^{3+} ion, respectively. In the Pr-rich solution region with formula $Ca_{3y/2}Pr_{(10-3y)/3}Cu_5O_{10}$ the unit cell volume also decreases with the increase of the Pr content. Since the content of oxygen is kept constant in the unit formula and the total number of (Ca + Pr) in the unit cell is reduced with increasing the Pr content, there exists a deficiency of Ca or Pr due to valence neutrality in the solid solution, leading to the decreasing unit cell volume.

The crystal structure of $Ca_{2.4}Pr_{1.6}Cu_5O_{10}$ compound was determined by the X-ray powder diffraction. The X-ray powder diffraction data of $Ca_{2.4}Pr_{1.6}Cu_5O_{10}$ are listed in Table 4. They can be indexed by a monoclinic cell. We use monoclinic supercell "B" with parameters $a = 14.123(2)$ Å, $b = 6.3693(5)$ Å, $c = 15.543(1)$ Å, $\beta = 136.60(1)°$ to analyze the crystal structure of $Ca_{2.4}Pr_{1.6}Cu_5O_{10}$. The reflections appear only when $l = 2n$ for (h0l) and $k = 2n$ for (0k0). According to these systematic reflection conditions, its space group is exclusively assigned as $C_{2h}^5 - P2_1/c$.

The crystal structure of $Ca_{2.4}Pr_{1.6}Cu_5O_{10}$ is isostructural to $Ca_2Y_2Cu_5O_{10}$ [29]. There are 4 formula unit per unit cell, i.e., each unit cell contains 9.6 Ca + 6.4 Pr + 20 Cu + 40 O. It is supposed that atoms Ca and Pr are distributed disorderly, 16 (Ca + Pr), 20 Cu and 40 O occupy four 4(e), five 4(e) and ten 4(e) equivalent sites of space group $P2_1/c$, respectively. The Rietveld method is used to refine the atomic parameters of the crystal structure of $Ca_{2.4}Pr_{1.6}Cu_5O_{10}$ by using DBWS-9411 program [26]. The initial atomic parameters were based

but δl decreases. For the sample with nominal composition $Ca_{1.6}Pr_{2.4}Cu_5O_{10}$ the split superstructure pair of reflections has converged to one reflection (see Fig. 3), $\delta l = 0$ and $\beta = 90°$.

The variation of the subcell lattice parameters a, b, c and V with composition in the $Ca_2Pr_2Cu_5O_{10}$-based solid solution is shown in Fig. 5. It can be observed that in the Ca-rich region the lattice parameters a, b, c and the volume of the unit cell V decrease when the Ca content increases; in the Pr-rich region the lattice parameters b and c are kept nearly constant, but the lattice parameters a and V decrease with the increasing Pr content. The unit cell volume reaches a maximum value at the ideal composition $Ca_2Pr_2Cu_5O_{10}$. In the Ca-rich solid solution region with formula
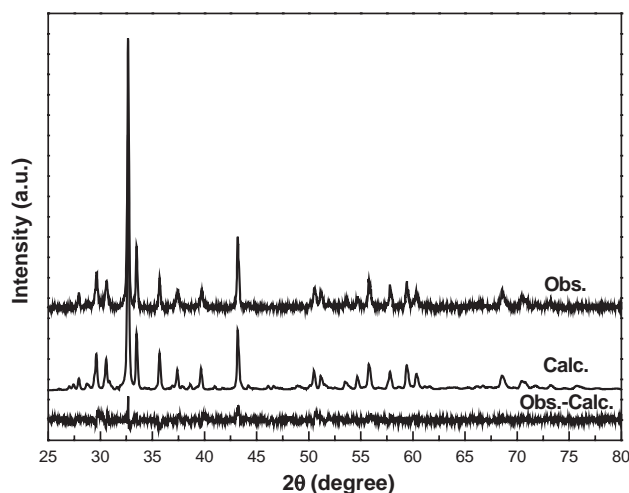

Fig. 6. The observed (upper), calculated (middle) and difference (on bottom) X-ray diffraction patterns for sample $Ca_{2.4}Pr_{1.6}Cu_5O_{10}$.

Table 5
Atomic parameters of $Ca_{2.4}Pr_{1.6}Cu_5O_{10}$ (space group $P2_1/c$)

Atoms	Position	x	y	z	occupancy	ΣV
Cu(1)	4e	0.3544(4)	0.5137(1)	0.7581(4)	1	1.97
Cu(2)	4e	0. 4401(3)	0.0030(2)	0.7390(4)	1	2.00
Cu(3)	4e	0.7605(0)	0.4857(6)	0.7488(5)	1	1.96
Cu(4)	4e	0.8555(3)	0.0096(1)	0.7547(2)	1	1.96
Cu(5)	4e	0.9421(5)	0.4726(1)	0.7499(1)	1	1.96
Pr(1)	4e	0.4344(1)	−0.7494(1)	0.5047(4)	0.4	2.93
Ca(1)	4e	0.4344(1)	−0.7494(1)	0.5047(4)	0.6	
Pr(2)	4e	−0.6290(3)	0.7611(1)	−0.9881(1)	0.4	2.93
Ca(2)	4e	−0.6290(3)	0.7611(1)	−0.9881(1)	0.6	
Pr (3)	4e	0.8799(1)	−0.7563(3)	0.9933(2)	0.4	2.96
Ca(3)	4e	0.8799(1)	−0.7563(3)	0.9933(2)	0.6	
Pr(4)	4e	−0.1783(0)	0.7466(6)	0.0092(1)	0.4	2.93
Ca(4)	4e	−0.1783(0)	0.7466(6)	0.0092(1)	0.6	
O(1)	4e	0.0500	0.5000	0.3750	1	2.32
O(2)	4e	0.1500	0.0000	0.3750	1	1.82
O(3)	4e	0.2500	0.5000	0.3750	1	2.41
O(4)	4e	0.3500	0.0000	0.3750	1	2.22
O(5)	4e	0.4500	0.5000	0.3750	1	2.15
O(6)	4e	0.5500	0.0000	0.3750	1	2.29
O(7)	4e	0.6500	0.5000	0.3750	1	2.02
O(8)	4e	0.7500	0.0000	0.3750	1	2.38
O(9)	4e	0.8500	0.5000	0.3750	1	1.84
O(10)	4e	0.9500	0.0000	0.3750	1	1.84

Note: The temperature factors of (Pr, Ca), Cu and O are fixed at $0.5\,\text{Å}^2$, $0.7\,\text{Å}^2$ and $1\,\text{Å}^2$, respectively. ΣV—bond-valences of ions.

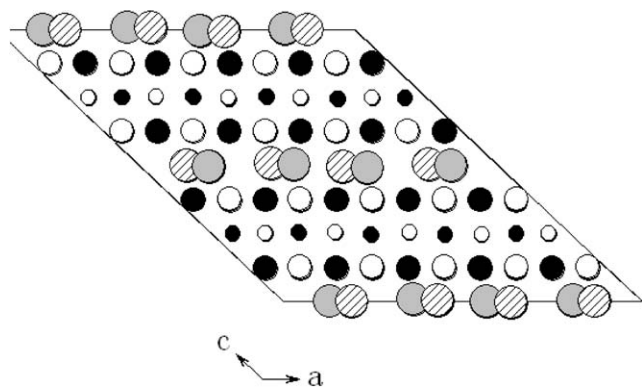Fig. 7. Crystal structure of $Ca_{2.4}Pr_{1.6}Cu_5O_{10}$ in projection alone the *b*-axis.

on the ideal position of $Ca_2Y_2Cu_5O_5$ structure [29]. The refinement result (see Fig. 6) shows a good agreement between the experimental and the calculated patterns with $R_P = 4.16\%$, $R_{WP} = 5.36\%$, $R_{exp} = 2.10\%$. The final atomic parameters are listed in Table 5. The results of structure analysis indicate that the content of oxygen in unit cell cannot exceed 40 atoms. The projection of the crystal structure of $Ca_{2.4}Pr_{1.6}Cu_5O_{10}$ along the *b*-axis is shown in Fig 7. The calculated diffraction intensities by program LAZY are listed in Table 4.

The oxygen ions distribute on $y = 0$ and $1/2$ planes, copper ions deviate slightly from $y = 0$ to $1/2$. Each copper ion is coordinated to 4 oxygen ions and form an infinite $[CuO_{4/2}]$ chain along the *a*-axis. The (Ca, Pr) ions locate on planes at $y \approx 1/4$ and $3/4$ between $[CuO_{4/2}]$ chains. (Ca, Pr) ion and 6 oxygen ions form a distorted octahedron. The structure of $Ca_{2.4}Pr_{1.6}Cu_5O_{10}$ contain an infinite one-dimensional chain of edge-shared square planar cuprate groups crosslinked by cations Ca and Pr, which occupy sites in the interchain tunnels.

The bond–valences of (Ca, Pr), Cu and oxygen are calculated by Brown's empirical bond valence method [27,28] according to the bond lengths of cation-oxygen listed in Table 5. Their bond–valences basically coincide with their normal chemical values, indicating that the crystal structure of $Ca_{2.4}Pr_{1.6}Cu_5O_{10}$ is reasonable.

4. Conclusions

The subsolidus phase relations of the PrO_x–CaO–CuO pseudo-ternary system sintered at 950–1000°C have been investigated by X-ray powder diffraction. In this system, there exist one compound $Ca_{10}Pr_4Cu_{24}O_{41}$ and one $Ca_2Pr_2Cu_5O_{10}$-based solid solution. The system can be divided into seven three-phase regions and two two-phase regions.

The crystal structures of $Ca_{10}Pr_4Cu_{24}O_{41}$ and $Ca_2Pr_2Cu_5O_{10}$-based solid solution have been determined. Compound $Ca_{10}Pr_4Cu_{24}O_{41}$ crystallizes in an orthorhombic cell with space group $D_{2h}^{20} - Cccm$, $Z = 4$. Its lattice parameters are $a = 11.278(2)\,\text{Å}$, $b = 12.448(3)\,\text{Å}$ and $c = 27.486(7)\,\text{Å}$. The crystal structure

of $Ca_2Pr_2Cu_5O_{10}$-based solid solution is an incommensurate phase based on the orthorhombic $NaCuO_2$-type subcell. The lattice parameters of $Ca_{2.4}Pr_{1.6}Cu_5O_{10}$ subcell are $a_0 = 2.8246(7)$ Å, $b_0 = 6.3693(5)$ Å, $c_0 = 10.679(1)$ Å, and its orthorhombic superstructure is with $a = 5a_0$, $b = b_0$, $c = 5c_0$. The $Ca_{2.4}Pr_{1.6}Cu_5O_{10}$ structure is also determined by using a monoclinic supercell with space group $C_{2h}^5 - P2_1/c$, $Z = 4$, $a = 5a_0$, $b = b_0$, $c = c_0/\sin \beta$ and $\beta = 104.79(1)^\circ$ or $136.60(1)^\circ$, $V = 5a_0b_0c_0$.

Acknowledgments

References

[1] J.G. Bednorz, K.A. Muller, Z. Phys. B- Condens. Matter 64 (1986) 189.

[2] M.K. Wu, J.R. Ashburn, C.J. Torng, P.H. Hor, R.L. Meng, L.J. Huang, Y.Q. Wang, C.W. Chu, Phys. Rev. Lett. 58 (1987) 908.

[3] Z.X. Zhao, L.Q. Chen, Q.S. Yang, Y.Z. Huang, G.U. Chen, R.M. Tang, C.G. Liu, L. Chen, Kexue Tongbao 32 (1987) 681.

[4] D.G. Hinks, L. Soderholm, D.W. Caponell, J.D. Jorgense, I.K. Schuller, C.U. Segre, K. Zhang, J.D. Grace, Appl. Phys. Lett. 50 (1987) 1688.

[5] P. Marsh, R.M. Fleming, M.L. Mandich, A.M. Desantolo, J. Kwo, M. Hong, L.J. Martinez-Miranda, Nature 334 (1988) 141.

[6] P. Bordet, C. Chaillout, J. Chenavas, J.L. Hodeau, M. Marezio, J. Karpinski, E. Kaldis, Nature 334 (1988) 569.

[7] M.B. Maple, Y. Dalichaouch, J.M. Ferreira, R.R. Hake, B.W. Lee, J.J. Neumeier, M.S. Torikachvili, K.N. Yang, H. Zhou, R.P. Guertin, M.V. Kuric, Physics B 148 (1987) 155.

[8] D.E. Morris, J.H. Nickel, J.Y.T. Wei, N.G. Asmar, J.S. Scoot, U.M. Scheven, C.T. Hultgren, A.G. Markely, Phys. Rev. B 39 (1989) 7347.

[9] T. Kogure, R. Kontra, G.J. Yurek, J.B.V. Sandel, Physica C 156 (1988) 45.

[10] D.E. Morris, N.G. Asmar, J.Y.T. Wei, J.H. Nickel, R.L. Sid, J.S. Scott, J.E. Post, Phys. Rev. B 40 (1989) 11406.

[11] Y.S. Yao, Y.F. Xiong, D. Jin, I.W. Li, F. Wu, J.K. Luo, Z.X. Zhao, Physica C 282–287 (1997) 49.

[12] K.Q. Li, Y.S. Yao, D.H. Cao, G.C. Che, S.L. Jia, Y.M. Ni, C. Dong, Z.X. Zhao, Physica C 341–348 (2000) 583.

[13] G.B. Song, J.K. Liang, L.T. Yang, J.R. Chen, G.Y. Liu, H.F. Yang, G.H. Rao, Appl. Phys. A 77 (2003) 915.

[14] H. Haas, E. Krdes, Z. Kristallogr. 129 (1969) 259.

[15] J. Gopalkrishnam, M.A. Subramanian, C.C. Torradi, J.P. Attfield, A.W. Sleight, Mater. Res. Bull. 24 (1989) 321.

[16] P.A. Tikhonov, M.V. Kravchinskaya, A.K. Kuznetsov, A.A. Safonov, E.F. Zhikhareva, Inorg. Mater. 19 (1983) 1887 (in Russian).

[17] C.L. Teske, H. Muller-Buschbaum, Z. Anorg. Allg. Chem. 370 (1970) 134.

[18] N. Kobayashi, Z. Hiroi, M. Takano, J. Solid State Chem. 132 (1997) 274.

[19] J.K. Liang, J. Chen, F. Wu, S.S. Xie, Solid State Commun. 75 (1990) 247.

[20] A.M.M. Gadalla, J. White, In: E. M. Levin, C.R. Robbins, H.F. Phase (Eds.), Diagrams for Ceramist, 2nd Edition, Fig. 2105, Amer. Ceramic. Soc., Columbus, 1969 (Mcmurdie).

[21] N.E. Brese, M. Okeeffe, R.B. VonDreele, V.G. Young, J. Solid State Chem. 83 (1989) 1.

[22] T. Siegrist, R.S. Roth, C.J. Rawn, J.J. Ritter, Chem. Mater. 2 (1990) 192.

[23] J. Pickardt, W. Paulus, M. Schmalz, R. Schollhorn, J. Solid State Chem. 89 (1990) 308.

[24] P.E. Werner, J. Appl. Cryst. 9 (1976) 216; P.-E. Werner, L. Eriksson, M. Westdahl, J. Appl. Cryst. 18 (1985) 367.

[25] E.M. McCarron Ø, M.A. Subramanian, J.C. Calabrese, R.L. Harlow, Mater. Res. Bull. 23 (1988) 1355.

[26] R.A. Young, A. Sakthivel, T.S. Moss, C.O. Paive-Santos, J. Appl. Cryst. 28 (1995) 366.

[27] I.D. Brown, in: M. O'Keeffe, A. Navrotsky (Eds.), Structure and Bonding in Crystals II, Academic Press, New-York, 1981, pp. 1–30.

[28] N.E. Brese, M. O'Keeffe, Acta Crystallogr. B 47 (1991) 192.

[29] P.K. Davis, J. Solid State Chem. 95 (1991) 365.

[30] C.Q. Han, G.B. Song, X.L. Chen, J.K. Liang, G.H. Rao, J. Solid State Chem. 173 (2003) 164.